

Methylation Microarray Analysis of Late-Stage Ovarian Carcinomas Distinguishes Progression-free Survival in Patients and Identifies Candidate Epigenetic Markers¹

Susan H. Wei, Chuan-Mu Chen,
Gordon Strathdee, Jaturon Harnsomburana,
Chi-Ren Shyu, Farahnaz Rahmatpanah,
Huidong Shi, Shu-Wing Ng, Pearly S. Yan,
Kenneth P. Nephew, Robert Brown, and
Tim Hui-Ming Huang²

Department of Pathology and Anatomical Sciences, Ellis Fischel Cancer Center [S. H. W., F. R., H. S., P. S. Y., T. H.-M. H.] and Department of Computer Engineering and Computer Science [J. H., C.-R. S.], University of Missouri, Columbia, Missouri 65203; Department of Zoology, National Chung Hsing University, Taiwan, Republic of China [C.-M. C.]; Cancer Research Campaign Department of Medical Oncology, Cancer Research Campaign Beatson Laboratories, University of Glasgow, Glasgow G61 1BD, United Kingdom [G. S., R. B.]; Department of Obstetrics and Gynecology and Reproductive Biology, Brigham and Women's Hospital, Harvard Medical School, Boston, Massachusetts 02115 [S.-W. N.]; and Medical Sciences, Indiana University School of Medicine, Bloomington, Indiana 47405 [K. P. N.]

ABSTRACT

Purpose: The purpose of this study was to profile methylation alterations of CpG islands in ovarian tumors and to identify candidate markers for diagnosis and prognosis of the disease.

Experimental Design: A global analysis of DNA methylation using a novel microarray approach called differential methylation hybridization was performed on 19 patients with stage III and IV ovarian carcinomas.

Results: Hierarchical clustering identified two groups of patients with distinct methylation profiles. Tumors from group 1 contained high levels of concurrent methylation, whereas group 2 tumors had lower tumor methylation lev-

els. The duration of progression-free survival after chemotherapy was significantly shorter for patients in group 1 compared with group 2 ($P < 0.001$). Differential methylation in tumors was independently confirmed by methylation-specific PCR.

Conclusions: The data suggest that a higher degree of CpG island methylation is associated with early disease recurrence after chemotherapy. The differential methylation hybridization assay also identified a select group of CpG island loci that are potentially useful as epigenetic markers for predicting treatment outcome in ovarian cancer patients.

INTRODUCTION

Ovarian cancer has the highest mortality rate of the reproductive cancers and is the fourth leading cause of cancer death in women (1). Because this cancer is often asymptomatic in its early stages, most patients are diagnosed at the late stages of III and IV, and 5-year survival for patients with advanced disease is <20% (1). There has been little change in ovarian cancer incidence and mortality over the past 30 years. Although a variety of tumor markers are available for monitoring ovarian cancer, their clinical utility remains unclear, and many individual markers are limited in specificity or sensitivity (2). Toward comprehensive diagnosis and prognosis of ovarian and other cancers, multiple molecular approaches are being used, such as cDNA microarrays to profile changes in gene expression levels and identify potential biomolecular markers (3). Aberrant DNA methylation is a frequent epigenetic event in ovarian cancer (4, 5) that represents an additional source of molecular markers. Through the addition of a methyl group to the cytosine of a CpG dinucleotide, this aberrant event occurs often in multiple CpG islands located in the promoter and first exon of genes and has been implicated in gene silencing during tumor development (see recent reviews in Refs. 6 and 7). For high-throughput screening of methylated CpG islands in tumors, a method called DMH³ was devised in our laboratory (8) and has since been further developed for large-scale, global analysis using microarray technology (9). In the present study, DMH was used to investigate CpG island hypermethylation across stage III and IV ovarian tumors. Hierarchical clustering revealed two tumor groups with distinctly different methylation profiles. Furthermore, patients defined by these groups differed markedly in the time until disease recurrence after chemotherapy. This differential methylation was independently confirmed by MSP, yielding

Received 1/15/02; revised 4/2/02; accepted 4/15/02.

The costs of publication of this article were defrayed in part by the payment of page charges. This article must therefore be hereby marked *advertisement* in accordance with 18 U.S.C. Section 1734 solely to indicate this fact.

¹ Supported in part by National Cancer Institute Grants CA-69065 and CA-86701 (to T. H.-M. H.), the United Kingdom Cancer Research Campaign (G. S. and R. B.), and the Gynecologic Oncology Group Grant through NIH CA27469 (K. P. N.). S. H. W. was supported by a postdoctoral fellowship from the Cancer Research Center, Inc. (Columbia, MO). C.-M. C. was a visiting fellow supported by the National Science Council, Taiwan (NSC39073F). T. H.-M. H. is a consultant to Epigenomics, Inc.

² To whom requests for reprints should be addressed, at Department of Pathology and Anatomical Sciences, Ellis Fischel Cancer Center, University of Missouri, 115 Business Loop I-70 West, Columbia, MO 65203. Phone: (573) 882-1276; Fax: (573) 884-5206; E-mail: huangh@health.missouri.edu.

³ The abbreviations used are: DMH, differential methylation hybridization; MSP, methylation-specific PCR; BSFS, batch sequential forward selection; PFS, progression-free survival.

Table 1 Clinicopathological information for the ovarian tumors

| Patient no. ^a | Clinical stage | Tumor histology | Specimen | Chemotherapy | PFS (mo) ^b |
|--------------------------|----------------|--------------------------------|----------|--|-----------------------|
| O2 | III | PD ^c adenocarcinoma | Primary | Carboplatin, Taxol | 7 |
| O86 | IIIc | MD | Primary | Carboplatin, Taxol | 7 |
| O37 | IV | NA | Primary | Carboplatin, docetaxol, epirubicin | 4 |
| AN2 | IIIa | SP, adenocarcinoma | Primary | Taxol, cisplatin, etoposide, topotecan | NA ^d |
| 20T | IIIc | SP, adenocarcinoma | Primary | Carboplatin, Taxol | 4 |
| O99 | III | SP, PD | Relapse | Cyclophosphamide, melphalan | (<8) |
| O8 | III | Malignant granulosa cell | Relapse | Cyclophosphamide, cisplatin, doxorubicin | (<6) |
| O5 | III | PD adenocarcinoma | Relapse | Chlorambucil | 5 |
| O98 | III | PD | Relapse | Cyclophosphamide, carboplatin | 14 |
| 12T | IIIc | SP, adenocarcinoma | Primary | Cisplatin, Taxol | 60 |
| O44 | IV | SP, adenocarcinoma | Primary | Carboplatin, Taxol | 20 |
| 26T | IV | SP, adenocarcinoma | Primary | Carboplatin, Taxol | 39 |
| O100 | IV | MD | Relapse | Carboplatin, treosulfan | 12 |
| O56 | IIIc | PD | Primary | Carboplatin, docetaxol, epirubicin | 16 |
| AN3 | IIIc | Serous, adenocarcinoma | Primary | Cytosan, carboplatin | (<9) |
| 10T | IIIc | SP, adenocarcinoma | Primary | Cisplatin, Taxol | 12 |
| 1T | IIIc | SP, adenocarcinoma | Primary | Melphalan | (60) |
| O60 | IIIc | SP, PD | Primary | Carboplatin | 12 |
| O34 | IV | SP | Primary | Carboplatin | 15 |

^a Grouped together following hierarchical clustering analyses (see text for details).

^b Where PFS data were unavailable, overall survival times are listed in parentheses.

^c PD, poorly differentiated; MD, moderately differentiated; SP, serous papillary.

^d NA, not available.

a select group of CpG island loci that may be useful as epigenetic markers for predicting chemotherapy outcome in patients with ovarian cancer.

MATERIALS AND METHODS

Tissue and DNA Samples. Eighteen advanced epithelial ovarian tumors and one granulosa cell tumor were obtained from the Cooperative Human Tissue Network (Columbus, OH), Western Infirmary and Stobhill General Hospital (Glasgow, United Kingdom), Pembury Hospital (Kent, United Kingdom), and Brigham and Women's Hospital (Boston, MA). All tumor specimens were examined and classified by institutional pathologists. Normal ovarian tissue could not be obtained from these patients for use as a control. However, 11 uninvolved, normal tissue samples adjacent to the ovarian tumors were obtained. Where corresponding normal tissue was not available for pairing with a tumor, a mixture of the normal tissues was used as the reference. This study was approved by local institutional review boards or ethics committees. Clinicopathological information on these ovarian tumors is listed in Table 1. Genomic DNA was extracted from these specimens using the QIAamp tissue kit (Qiagen).

CpG Island Microarray. The microarray panel of 7776 CpG island loci was derived from a genomic library, CGI (10), made available through the Human Genome Mapping Project Resource Centre, United Kingdom. PCR products (0.2–2 kb, ~0.02 μl/dot, and 0.1 μg/μl) in 20% DMSO were directly spotted as 150-μm-diameter microdots spaced 300 μm apart on poly-L-lysine-coated glass slides using an Affymetrix/GMS 417 arrayer, which does not require purified products because its ring-and-pin system is much less susceptible to clogging than the common quill- or inkjet-type printing heads. The arrayed slides were processed and denatured before use according to

DeRisi *et al.*⁴ For internal controls, 10 *MseI* genomic fragments that do not have the test methylation-sensitive sites and 6 *MseI* exonic fragments for the genes β -actin, GAPDH, and DFR were also spotted on the glass slides.

Amplicon Generation. Preparation of tumor and normal amplicons was performed as described previously (9). Briefly, 2 μg of DNA were digested with *MseI* and ligated to the annealed linkers H-12 (5'-TAA-TCC-CTC-GGA) and H-24 (5'-AGG-CAA-CTG-TGC-TAT-CCG-AGG-GAT) using the Fast-Link DNA ligation kit (Epicentre). Then, the sample was restricted with methylation-sensitive endonucleases *Bst*UI and *Hpa*II (New England Biolabs) and amplified by PCR from the H-24 linker. Amplification was carried out for 20 cycles under conditions described previously (9). The amplified products (or amplicons) were purified for labeling with cyanine dyes.

Microarray Hybridization. Differential hybridization was conducted using the CpG island microarray panel. Tumor and normal control amplicons were first labeled with amino-allyl-dUTP using the BioPrime DNA kit (Life Technologies, Inc.) and coupled with fluorescent dyes Cy5 and Cy3 (Amersham-Pharmacia Biotech), respectively. Where available, tumor amplicon was cohybridized with its paired normal amplicons (11 cases). In the other cases, pooled DNA from six normal tissue samples was used to prepare a control amplicon. Hybridization and posthybridization washing protocols were as described by DeRisi *et al.*,⁴ which involved an overnight hybridization step at 60°C in a HybChamber (GeneMachines). After washing and drying, the slides were scanned with a GenePix

⁴ www.microarrays.org.

Table 2 Primer sequences of seven CpG island loci and reaction conditions used for MSP

Amplification was carried out in 20–25- μ l volumes of reaction containing 10 mM Tris-HCl (pH 8.3), 50 mM KCl, 1.5 mM MgCl₂, 10 mM deoxynucleotide triphosphates, 0.25–0.3 μ M primers, 20–25 ng of bisulfite-treated DNA, and 0.5 units of AmpliTaq Gold DNA polymerase. PCR was performed with 1 cycle of 95°C for 10 min, 35 cycles of 94°C for 45–60 s, annealing at the indicated temperature for 45–60 s, and 72°C for 45–90 s, followed by 1 cycle of 72°C for 5 min.

| Clone | | Upstream primer 5'→3' | Downstream primer 5'→3' | Annealing temperature (°C) | Size (bp) |
|----------|----------------|---------------------------------|---------------------------------|-------------------------------|--------------|
| CpG15G2 | M ^a | ATACCCTATAACTCCTTTTAAAACTCGAA | CGCGGACGTTTGTAGTTAAGGTTTC | 59 | 133 |
| | U | CAACAAACCTTAACTAAACATCCACAAAA | GGGTAATATTTAAGATTGTGTGTTGATGT | 54 | 138 |
| CpG13B8 | M | TGTTTTTAGGGTTGGTTTTTAATCGTTC | GACCGAATTCAACTTCGCCG | 62 | 174 |
| | U | TTTTAGGGTTGGTTTTTAATGTTT | AAACCAAATTCAACTTCACCA | 55 | 174 |
| SC22B8 | M | AGGTGTGAGGTTTACGTATTTTGTAGTTAC | ACGACGATACGAATAAAAAAACG | 56 | 165 |
| | U | GAGGTGTGAGGTTTATGTATTTTGTAGTTAT | CCAACAACAATACAAATAAAAAAACA | 54 | 169 |
| SC13D6 | M | AATAAACTCCTACATCGGAAAAAACG | TTTTCGTGTCGGGTTTTGTGTTTTTC | 59 | 171 |
| | U | GATTTTTGTATTTGTGGAGAAGTG | ATCACCCCTACATCCCTCCTCA | 54 | 181 |
| SC5E7 | M | CTCGCTCGCTCCTACTCGCTATCG | AATTCGGAAAAACGTAGTTTTTTTTAAAGAA | 60 | 180 |
| | U | ACCTCACTCACTCCTACTCACTATCA | AATTTGGAAAAATGTAGTTTTTTTTAAAGAA | 56 | 181 |
| CpG12D5 | M | AGGTTAAACGAGTTTTTTCGGGTTTC | ATCAAAAATCCATTTTATTAACAAAAACG | 58 | 141 |
| | U | GAATAGGTTAAATGAGTTTTTTCGGGTTT | AATCAAAAATCCATTTTATTAACAAAAACA | 56 | 146 |
| CpG28F11 | M | AAACTAAAAAAAACAAAACCGCGAACGAA | GGTTTGACGGGGCGCGTTTC | 62 | 113 |
| | U | CACCTCAATTCCAATTTACATCCTACCA | TGTATGGTTGTATGGGGTGTGTTTTGT | 62 | 235 |

^a M, methylated; U, unmethylated.

4000A scanner (Axon), and the images were analyzed with GenePix Pro 3.0.

Data Analysis. The Cy5: Cy3 ratio of a microarray spot was a measure of the methylation difference between tumor and normal amplicons for a given CpG island locus. For each spot, the net pixel intensity was determined by subtracting a local background. To correct for hybridization variations, a global normalization factor determined by the median Cy5: Cy3 ratio of the microarray panel was applied. Loci with hybridization intensities near to the background or containing repetitive sequences were excluded from this calculation. The normalization factor was evaluated against the internal controls whose Cy5: Cy3 ratios were expected to be 1. Each spot was adjusted accordingly using the derived normalization factor, and a new Cy5: Cy3 ratio was generated. The data set was then log-transformed and analyzed using Eisen's hierarchical clustering package.⁵ Clustering was carried out using the Pearson correlation coefficient as the distance metric, and the clusters were agglomerated using the complete linkage criterion. In general, tumors bearing similar methylation profiles clustered together. A BSFS algorithm was next applied to clinical features that correlated with the clustering results using the initial dataset (see "Results"). This algorithm was used to select for loci that most discriminated between two subgroups identified in the initial analysis. The scoring algorithm S is as follows, where the variable V is a binary vector for each clone:

$$S = \frac{\min(V_{High}^{Gene}, V_{High}^{ideal})}{\max(|V_{High}^{Gene}|, |V_{High}^{ideal}|)} + \frac{\min(V_{Low}^{Gene}, V_{Low}^{ideal})}{\max(|V_{Low}^{Gene}|, |V_{Low}^{ideal}|)}$$

The measured values (S) represented high or low methylation levels of loci in experimental and ideal cases. A separate log-rank test was used to compare PFS with the main clusters

identified from DMH. The methylation status analysis was performed blinded to clinical outcome, and, conversely, PFS was determined blinded to methylation status.

MSP. The methylation status of seven CpG island loci (*CpG15G2*, *CpG13B8*, *SC22B8*, *SC13D6*, *SC5E7*, *CpG12D5*, and *CpG28F11*) in ovarian tumors and normal controls was determined by MSP, essentially as described by Herman *et al.* (11). The primer sets designed for the methylated and unmethylated DNAs for each CpG island locus are listed in Table 2. All PCR reactions were performed on PTC-100 thermocyclers (MJ Research) and in 20–25- μ l volumes using AmpliTaq Gold DNA polymerase (Perkin-Elmer). In subsequent analysis, loci were determined to be completely methylated (score of 1; an amplified product detected using the methylated but not the unmethylated primer set), partially methylated (score of 0.5; PCR products detected using both the methylated and unmethylated primer sets), or completely unmethylated (scored as 0; an amplified product detected using the unmethylated but not the methylated primer set; see examples in Fig. 2A). Cox regression analysis was used to test the relationship between PFS and methylation status determined by MSP.

RESULTS

Identification of Hypermethylated CpG Island Clusters Associated with PFS in Patients by DMH. Of the 7776 CpG island tags probed by DMH amplicons from the 19 ovarian tumors, a total of 956 loci had normalized Cy5: Cy3 ratios of ≥ 1.5 and were considered to be hypermethylated in tumor relative to control. This is attributable to a greater abundance of methylated DNA fragments that resisted methylation-sensitive digestion in tumor samples and were amplified by linker PCR, whereas the same unmethylated, allelic fragments were restricted in normal samples and could not be amplified. These methylation differences were reflected in Cy5-labeled tumor and Cy3-labeled normal hybridization intensities in the microarray. Although it is likely that there are low amounts of residual

⁵ <http://rana.stanford.edu/clustering>.

normal stroma or infiltrating lymphocytes present in these tumor specimens, the presence of some normal cells in tumor samples did not seem to affect the DMH assay (8, 9). It is because the detection of hypermethylated sequences is for the presence of positive hybridization signals in tumor samples, but not in normal samples. The total number of hypermethylated loci ranged from 48–348 (0.6–4.6%) in this tumor group. The dataset was comprised of shared methylated loci across multiple tumors as well as uniquely methylated loci in individual tumors. The ratio cutoff of ≥ 1.5 identified hypermethylated loci with $\geq 90\%$ accuracy, which agrees with our previous DMH study using breast cancer samples (9) and Southern analyses using DMH amplicons as hybridization templates (data not shown, see also Ref. 9).

Hierarchical clustering of the 956 loci revealed two subgroups of ovarian tumors in this patient cohort: group 1 (8 tumors) had a mean of 237 ± 80 hypermethylated loci/tumor; whereas group 2 (11 tumors) exhibited fewer hypermethylated loci (102 ± 37 ; Fig. 1A). It was of interest to determine whether individual loci or a subset of loci could be correlated with patients' clinical outcome. Thus, a BSFS algorithm was used to select for hypermethylated loci within the 956 loci that were predominantly present in group 1 but not in group 2. The BSFS analysis revealed a subset of 182 hypermethylated loci for the two groups, showing definitively that more loci were hypermethylated per tumor in group 1 than in group 2 (105 ± 27 versus 13 ± 5 loci/tumor, respectively; Fig. 1B). This differential methylation in ovarian tumors correlated significantly ($P < 0.001$, log-rank test) with PFS, defined by the time of clinical disease recurrence after chemotherapy (Table 1). In general, group 1 patients had a PFS of < 8 months, whereas for group 2, with the exception of patient AN3, the PFS was 12 months or greater. The median PFS in group 1 was 6 months as compared with 15 months in group 2, representing a hazard ratio of 2.5. There was no association of methylation profiles with the status of clinical stage, tumor histology, or age at diagnosis of these patients.

Sequence characterization of the 182 loci preferentially hypermethylated in the group 1 tumors revealed CpG island sequences located in the promoter and the first exon of known genes (see representative examples in Fig. 1C). In addition, many hypermethylated loci were mapped to other exonic regions or genomic regions with no known gene functions.

Confirmation of the Association of CpG Island Hypermethylation with Clinical Parameters by MSP. MSP was conducted in 17 available ovarian tumors and 8 normal controls, and seven of the loci obtained using BSFS validated the association of hypermethylation with PFS (Fig. 2). Tumors from group 1 displayed higher methylation scores than those of group 2 (0.54 ± 0.2 versus 0.16 ± 0.15). Again, the methylation status of the seven markers in these tumors determined by MSP correlated significantly with PFS ($P = 0.0067$), consistent with the notion of two distinct subgroups based on the clustering analyses. Methylation of these loci was not detected in normal control samples.

It should be pointed out that MSP is more sensitive toward identifying methylated CpG sites one locus at a time, whereas DMH is for large-scale interrogation of extensively methylated loci. Therefore, the MSP and DMH data did not strictly corre-

late. For example, partial methylation of these seven loci was detected in O34, a tumor belonging to group 2 as determined by MSP, but could not be identified by DMH. Although we expected some minor inconsistencies using these two different approaches, they did not affect the overall interpretation of our results, given the large number of CpG island loci analyzed.

DISCUSSION

In this study using DMH to assess global methylation changes and MSP to validate the methylation findings, we showed that CpG island hypermethylation is widespread in ovarian cancer genomes, which is consistent with our early investigation (4, 5). One of the goals of this study was to examine the potential use of DMH to predict treatment outcome for ovarian cancer patients. A total of 956 hypermethylated CpG islands were identified by DMH in the ovarian tumors analyzed. Cluster analysis further demonstrated that 182 such loci were significantly associated with a clinical parameter, PFS, indicating that hypermethylated CpG islands may be an important prognostic marker for the disease (12).

As shown in Fig. 1C, sequences of several hypermethylated loci (e.g., *CpG12D5*, *CpG13B8*, *CpG28F11*, *SC13D6*, *SC22B8*, and *CpG16B4*, and so forth) matched the 5'-ends of known genes or cDNAs whose cellular functions include cell cycle progression, trophism, and cell development and differentiation. Future studies will be needed to determine how hypermethylation of their promoters resulting in transcriptional silencing may play a role in ovarian tumorigenesis. We also observed hypermethylation of many nonpromoter CpG islands in ovarian cancer. Nguyen *et al.* (13) have suggested that many nonpromoter CpG islands appear to be more susceptible to aberrant methylation than their nearby respective promoter sequences, where methylation can begin in exonic regions and then spread to CpG islands in other locations, including promoter regions. Therefore, nonpromoter hypermethylated loci could be used to indicate the relative location of genes that are more susceptible or fated to be inactivated by DNA hypermethylation. This can also lead to discovery of genes whose functions are indeed involved in ovarian cancer development.

The global presence of hypermethylation seems to correlate well with the advanced disease state and may conceivably be used in the overall assessment of ovarian cancer progression. It is reasonable to assume that only a subset of these loci play a critical role(s) in the tumorigenic process, which could be used to distinguish certain ovarian tumor types from others. As shown by the clustering analysis, we identified a panel of hypermethylated loci that are potential markers for identifying stage III or IV tumors with shorter PFS. Ovarian cancer patients with short PFS (< 1 year) have a poorer response to second-line therapies compared with patients with a PFS of > 1 year, suggesting that patients with shorter PFS have tumors that more readily acquire resistance to chemotherapy (14). In this regard, group 1 patients (PFS < 8 months) identified in this study may benefit from additional therapies at presentation or during remission. Because this patient cohort was a small sample size and had differences in treatment regimen, our results must be interpreted with caution. Although this was a preselected group of patients that is biased by the inclusion of the relapse tumors and

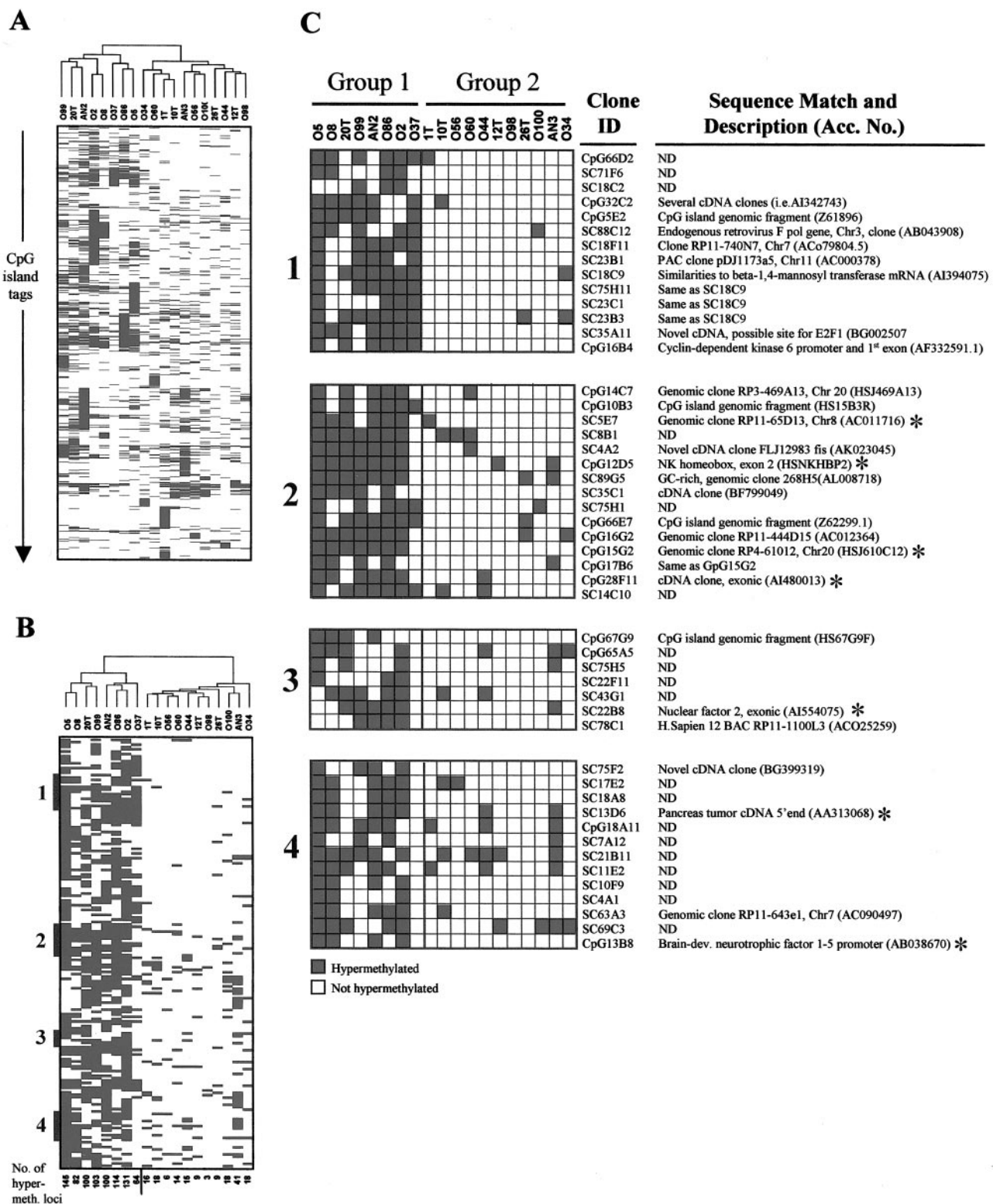


Fig. 1 Tumor profiling of 19 ovarian tumors by hierarchical clustering. A, unsupervised clustering of 956 unselected CpG island loci that are putatively hypermethylated as determined by DMH. B, BSFS of 182 CpG island loci that most discriminate between the two major subgroups of tumors. The BSFS algorithm measures the values of these loci in experimental and ideal cases for high degrees of methylation and, conversely, the values in experimental and ideal cases for low degrees of methylation. C, subclusters of CpG island loci separating group 1 and group 2 tumors. Sequence information for these loci is shown on the right. ND, not determined. Asterisks (*) indicate CpG island loci analyzed by MSP.

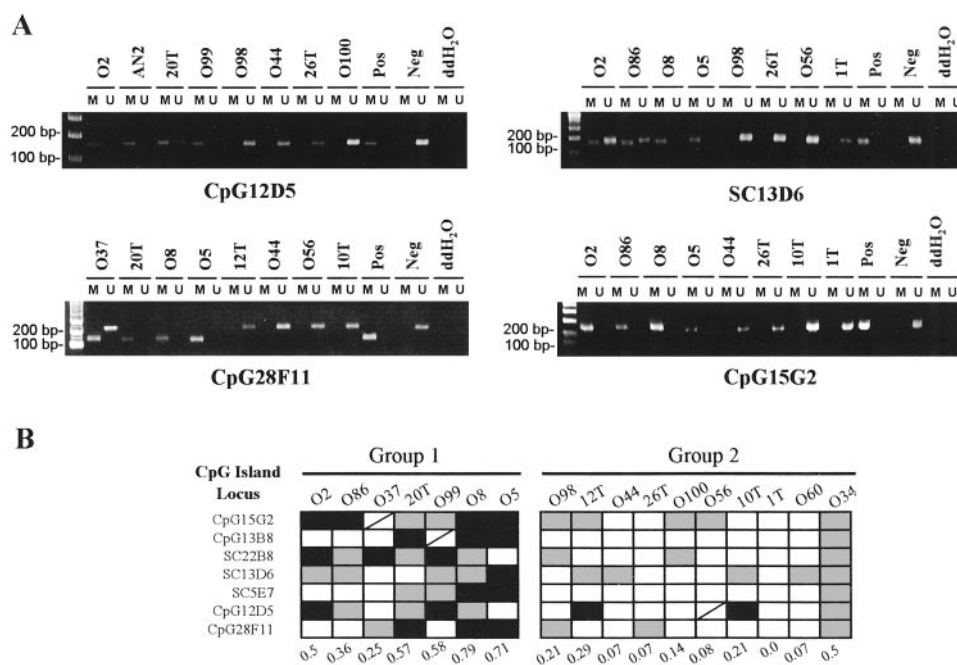


Fig. 2 Determination of hypermethylation of seven CpG island loci in ovarian tumors by MSP. **A**, representative results of four loci (*CpG12D5*, *SC13D6*, *CpG28F11*, and *CpG15G2*) by MSP. Positive (*Pos*) and negative (*Neg*) controls for the M primer set and U primer set were Universal Methylated DNA (Intergen) and human blood, respectively. For each tumor, 35 cycles of amplification were performed using primers for the methylated sequence (*M*) and unmethylated sequence (*U*) sets as described in the text. **B**, summary of 17 tumors examined by MSP. Tumors (groups 1 and 2) are listed on *top*, and CpG island loci are listed on the *right*. A slash (/) indicates that a PCR product could not be obtained with either of the methylated or unmethylated primer sets. The methylation status of a locus in a tumor was scored (completely methylated, 1 = black box; partially methylated, 0.5 = shaded box; or completely unmethylated, 0 = open box). The methylation score of each tumor is listed on the *bottom*.

assessed in a retrospective manner, these tumor samples were analyzed blinded to clinical outcome.

The present study lays the foundation for future analysis of ovarian cancer using this microarray-based technique. Our strategy will use a subpanel microarray containing the aforementioned 182 loci in a large prospective study. The recently constructed expressed CpG island sequence tag (ECIST) microarray panel can also be included to screen aberrantly hypermethylated loci and, at the same time, confirm their association with gene silencing in cancer cells (15). Furthermore, the development of novel therapies based on demethylation or agents that relieve chromatin repression is beginning for ovarian and other cancers (16, 17). Methylation profiling of ovarian tumors could therefore provide a means to identify patient populations who may particularly benefit from such approaches and form a rationale for new therapies designed to alter this fundamental process in ovarian cancer.

ACKNOWLEDGMENTS

We thank Dr. Charles W. Caldwell for helpful discussion, Jim Paul for statistical advice, Diane Peckham for assistance in the preparation of the manuscript, and the Scottish Gynecological Clinical Trials Group for tumor samples.

REFERENCES

1. Greenlee, R. T., Hill-Harmon, M. B., Murray, T., and Thun, M. Cancer statistics, 2001. *CA Cancer J. Clin.*, 51: 15–36, 2001.

- Meyer, T., and Rustin, G. J. Role of tumor markers in monitoring epithelial ovarian cancer. *Br. J. Cancer*, 82: 1535–1538, 2000.
- Welsh, J. B., Zarrinkar, P. P., Sapinoso, L. M., Kern, S. G., Behling, C. A., Monk, B. J., Lockhart, D. J., Burger, R. A., and Hampton, G. M. Analysis of gene expression profiles in normal and neoplastic ovarian tissue samples identifies candidate molecular markers of epithelial ovarian cancer. *Proc. Natl. Acad. Sci. USA*, 98: 1176–1181, 2001.
- Ahluwalia, A., Yan, P., Hurteau, J. A., Bigsby, R. M., Jung, S. H., Huang, T. H., and Nephew, K. P. DNA methylation and ovarian cancer. I. Analysis of CpG island hypermethylation in human ovarian cancer using differential methylation hybridization. *Gynecol. Oncol.*, 82: 261–268, 2001.
- Strathdee, G., Appleton, K., Illand, M., Millan, D. W., Sargent, J., Paul, J., and Brown, R. Primary ovarian carcinomas display multiple methylator phenotypes involving known tumor suppressor genes. *Am. J. Pathol.*, 158: 1121–1127, 2001.
- Baylin, S. B., Esteller, M., Rountree, M. R., Bachman, K. E., Schuebel, K., and Herman, J. G. Aberrant patterns of DNA methylation, chromatin formation and gene expression in cancer. *Hum. Mol. Genet.*, 10: 687–692, 2001.
- Jones, P. A., and Laird, P. W. Cancer epigenetics comes of age. *Nat. Genet.*, 21: 163–167, 1999.
- Huang, T. H.-M., Perry, M. R., and Laux, D. E. Methylation profiling of CpG islands in human breast cancer cells. *Hum. Mol. Genet.*, 8: 459–470, 1999.
- Yan, P. S., Chen, C.-M., Shi, H., Rahmatpanah, F., Wei, S. H., Caldwell, C. W., and Huang, T. H.-M. Dissecting complex epigenetic alterations in breast cancer using CpG island microarrays. *Cancer Res.*, 61: 8375–8380, 2001.

10. Cross, S. H., Charlton, J. A., Nan, X., and Bird, A. P. Purification of CpG islands using a methylated DNA binding column. *Nat. Genet.*, *6*: 236–244, 1994.
11. Herman, J. G., Graff, J. R., Myohanen, S., Nelkin, B., and Baylin, S. B. Methylation-specific PCR: a novel PCR assay for methylation status of CpG islands. *Proc. Natl. Acad. Sci. USA*, *93*: 9821–9826, 1996.
12. Widschwendter, M., and Jones, P. A. The potential prognostic, predictive and therapeutic values of DNA methylation in cancer. *Clin. Cancer Res.*, *8*: 17–21, 2002.
13. Nguyen, C., Liang, G., Nguyen, T. T., Tsao-Wei, D., Groshen, S., Lubbert, M., Zhou, J.-H., Benedict, W. J., and Jones, P. A. Susceptibility of nonpromoter CpG islands to *de novo* methylation in normal and neoplastic cells. *J. Natl. Cancer Inst. (Bethesda)*, *93*: 1465–1472, 2001.
14. Markman, M., and Bookman, M. A. Second-line treatment of ovarian cancer. *Oncologist*, *5*: 26–35, 2000.
15. Shi, H., Yan, P. S., Chen, C.-M., Rahmatpanah, F., Lofton-Day, C., Caldwell, C. W., and Huang, T. H.-M. Expressed CpG island sequence microarray for dual screening of DNA hypermethylation and gene silencing in cancer cells. *Cancer Res.*, *62*: 3124–3220, 2002.
16. Santini, V., Kantarjian, H. M., and Issa, J. P. Changes in DNA methylation in neoplasia: pathophysiology and therapeutic implications. *Ann. Intern. Med.*, *134*: 573–586, 2001.
17. Plumb, J. A., Strathdee, G., Sludden, J., Kaye, S. B., and Brown, R. Reversal of drug resistance in human tumor xenografts by 2'-deoxy-5-azacytidine-induced demethylation of the *hMLH1* gene promoter. *Cancer Res.*, *60*: 6039–6044, 2000.

Clinical Cancer Research

Methylation Microarray Analysis of Late-Stage Ovarian Carcinomas Distinguishes Progression-free Survival in Patients and Identifies Candidate Epigenetic Markers

Susan H. Wei, Chuan-Mu Chen, Gordon Strathdee, et al.

Clin Cancer Res 2002;8:2246-2252.

Updated version Access the most recent version of this article at:
<http://clincancerres.aacrjournals.org/content/8/7/2246>

Cited articles This article cites 17 articles, 6 of which you can access for free at:
<http://clincancerres.aacrjournals.org/content/8/7/2246.full#ref-list-1>

Citing articles This article has been cited by 21 HighWire-hosted articles. Access the articles at:
<http://clincancerres.aacrjournals.org/content/8/7/2246.full#related-urls>

E-mail alerts [Sign up to receive free email-alerts](#) related to this article or journal.

Reprints and Subscriptions To order reprints of this article or to subscribe to the journal, contact the AACR Publications Department at pubs@aacr.org.

Permissions To request permission to re-use all or part of this article, use this link
<http://clincancerres.aacrjournals.org/content/8/7/2246>.
Click on "Request Permissions" which will take you to the Copyright Clearance Center's (CCC) Rightslink site.